Thermal Stability of Nickel Silicide and Shallow Junction Electrical Characteristics with Carbon Ion Implantation

2010 Jpn. J. Appl. Phys. 49 04DA04

(http://iopscience.iop.org/1347-4065/49/4S/04DA04)

Thermal Stability of Nickel Silicide and Shallow Junction Electrical Characteristics with Carbon Ion Implantation

Bing-Yue Tsui* and Chen-Ming Lee

Department of Electronics Engineering and Institute of Electronics, National Chiao Tung University, Room ED641, No. 1001, Ta-Hsueh Road, Hsinchu, Taiwan 30010, R.O.C.

Received October 6, 2009; accepted December 21, 2009; published online April 20, 2010

In this work, we investigated the impact of carbon ion implantation on the thermal stability of nickel silicide film and nickel-silicide-contact n^+/p shallow junctions. A higher carbon ion implantation dose can prevent the nickel silicide film from agglomeration and phase transformation. However, good thermal stability does not necessarily lead to excellent junction current–voltage characteristics owing to the diffusion of nickel atoms. When the carbon ion implantation dose increases to $5 \times 10^{15}\,cm^{-2}$, many crystal defects are created. Then, numerous nickel atoms diffuse along these defects into the junction depletion region during the silicide formation process, resulting in poor junction characteristics. The trade-off between thermal stability and junction electrical characteristics is discussed in this paper. Finally, two methods are suggested to solve the serious leakage current problem.

DOI: 10.1143/JJAP.49.04DA04

1. Introduction

Nickel monosilicide (NiSi) has been extensively investigated and used as a source/drain (S/D) contact material for a long time. NiSi has several advantages including low resistivity, low contact resistivity, a low-temperature process, less Si consumption during silicide formation, no narrow-line effect, and no bridging failure.[1)] However, the main issue of NiSi film is its thermal stability at high temperatures. It is well known that NiSi film agglomerates to form small broken holes and then discontinuous islands at 700 °C, and the NiSi phase transforms into $NiSi_2$ phase at 700–750 °C. These two factors cause an increase in the sheet resistance (R_s) of the Ni-silicide film. Moreover, with the continuous scaling down of complementary metal–oxide–semiconductor (CMOS) devices, ultra shallow S/D junctions are becoming increasingly important in order to suppress the short-channel effect (SCE). The decrease in junction depth requires a decrease in NiSi film thickness, which has a strong effect on its thermal stability. Consequently, several methods of raising the thermal stability of NiSi film have been published.[2–7)] These methods involve ion implantation (I/I) utilizing F or N_2 ions before NiSi formation, the deposition of Ti or Pt as a capping layer or an interposing layer, and the deposition of a $Ni_{1-x}Ti_x$ or $Ni_{1-x}Pt_x$ alloy.

Recently, Zaima *et al.* have reported that a p^+ $Si_{0.996}C_{0.004}$ epitaxial layer grown by low-pressure chemical vapor deposition (LPCVD) can effectively raise the thermal stability of NiSi film,[8)] and similar results were also reported by Nakatsuka *et al.*[9)] The mechanism of suppressing the agglomeration and phase transformation of NiSi film is that C atoms segregate to the NiSi grain boundaries and NiSi/Si interface to modify the grain boundary and interfacial energy due to the low solid solubility of C atoms in NiSi.[10)] Two common methods have been used to include C atoms within a Si substrate. One is $Si_{1-x}C_x$ epitaxial growth directly on a Si substrate,[8,10)] and the other is C I/I into a Si wafer surface followed by thermal annealing.[9,11,12)] As a result of the extremely low solid solubility of C atoms in Si, the $Si_{1-x}C_x$ epitaxial process cannot easily achieve a higher substitutional C concentration than 1% ($x > 1\%$).[13)] In this work, we focus on C I/I technology. This process is simpler than the epitaxy process and is compatible with the standard CMOS process flow. Moreover, it has been demonstrated that a $Si_{1-x}C_x$ S/D can produce tensile strain in the channel region, increasing the electron mobility and drive current of n-type metal–oxide–semiconductor field-effect transistors (NMOSFETs).[14,15)] Thus, C I/I technology is feasible for integration with n^+/p shallow junctions in the future.

The impact of the C I/I process on n^+/p shallow junction current–voltage (I–V) characteristics has not been studied in detail. In this paper, we demonstrate and discuss the trade-off between the thermal stability of NiSi film and the n^+/p shallow junction I–V characteristics. Some methods of fabricating NiSi-contact n^+/p shallow junctions with both good thermal stability and excellent I–V characteristics are proposed.

2. Experiments

The starting material used in this study was a boron-doped (100) 6-in.-diameter Si prime wafer with a resistivity of 2–7 Ω cm. After typical local-oxidation-of-silicon (LOCOS) isolation, a 70-nm-thick screen oxide layer was thermally grown. Next, C ions were implanted through the screen oxide at 40 keV to a dose of 1×10^{15} or $5 \times 10^{15}\,cm^{-2}$. The projected range of C ions is 58 nm under the Si surface. Then, C I/I defects were eliminated by rapid thermal annealing (RTA) at 1100 °C for 30 s. Samples without C I/I were also prepared as reference. After etching the screen oxide by diluted HF (DHF) solution, arsenic (As) ions were implanted to a dose of $5 \times 10^{15}\,cm^{-2}$ at 35 or 85 keV followed by a 1050 °C spike annealing process. The lower As I/I energy of 35 keV results in more dopants within the Ni-silicide film and a shallower junction depth. After removing the native oxide by DHF solution, a 25-nm-thick Ni layer and a 5-nm-thick TiN capping layer were continuously deposited by a sputtering system followed by a two-step annealing process to form NiSi.[16)] The first step was performed at 300 °C for 60 min. After that, the TiN capping layer and the unreacted Ni were selectively removed by a mixture of $H_2O_2 : H_2SO_4 = 1 : 3$. The second annealing step was performed at a temperature of 500–800 °C for 30 s in order to study the NiSi thermal stability. Finally, a 500-nm-thick Al layer was deposited on the wafer backside surface by a sputtering system to complete the fabrication of the n^+/p shallow junctions. Blanket samples without a

*E-mail address: bytsui@mail.nctu.edu.tw

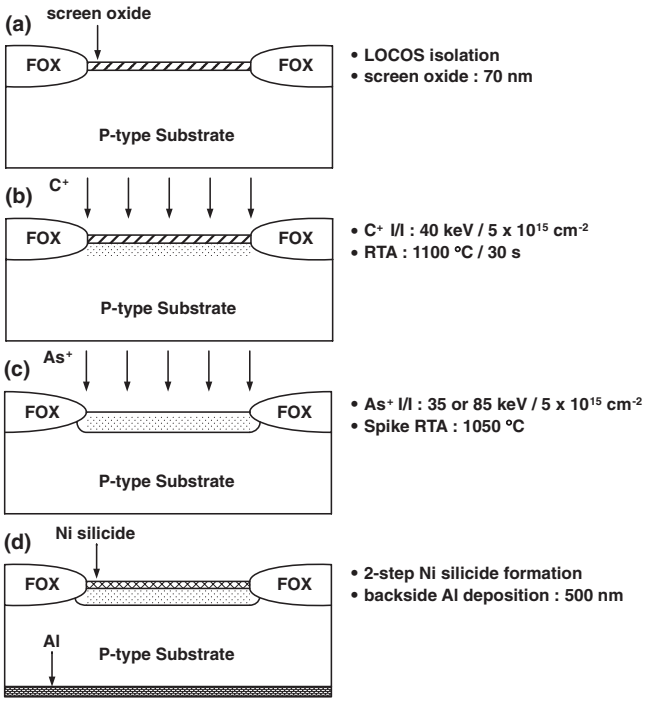

Fig. 1. Main process flow of the n^+/p shallow junction: (a) after LOCOS isolation and screen oxide growth, (b) after C I/I and annealing, (c) after As I/I and activation, and (d) the final structure.

Table I. Sample IDs and fabrication conditions of the Ni-silicide-contact n^+/p shallow junctions.

	Sample ID					
	C5As35	C5As85	C1As35	C1As85	C0As35	C0As85
C^+ dose (cm^{-2})	5×10^{15}	5×10^{15}	1×10^{15}	1×10^{15}	0	0
As^+ energy (keV)	35	85	35	85	35	85

LOCOS isolation structure were also fabricated for the purpose of material analysis. The main process flow of n^+/p shallow junctions is illustrated in Fig. 1. The notations used to identify different samples along with their fabrication conditions are summarized in Table I.

The four-point probe technique was used to measure the sheet resistance (R_s) of all samples with blanket Ni-silicide films. X-ray diffraction (XRD) was adopted to distinguish the NiSi phase from the $NiSi_2$ phase. Scanning electron microscopy (SEM) was used to inspect the surface morphology of the Ni-silicide. The I–V characteristics of the n^+/p shallow junctions were measured by an Agilent 4156C precision semiconductor parameter analyzer.

3. Results and Discussion

3.1 Thermal stability

Figure 2 shows the measured R_s values as a function of silicide formation temperature with As I/I energy at 35 keV. The samples with the higher C I/I dose of $5 \times 10^{15}\,cm^{-2}$ (C5As35) have slightly higher R_s values at a lower silicide formation temperature ($\leqq$700 °C) owing to the larger number of C atoms within the Ni-silicide film. Figures 3–5 display SEM images of the C0As35, C1As35, and C5As35 samples, respectively. The R_s values of the C0As35 samples

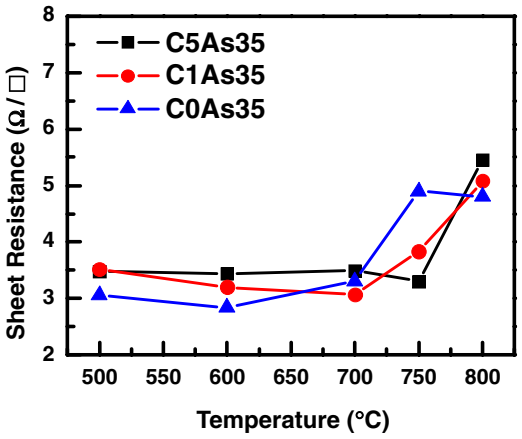

Fig. 2. (Color online) Sheet resistance values as a function of silicide formation temperature with As I/I energy at 35 keV and different C I/I doses.

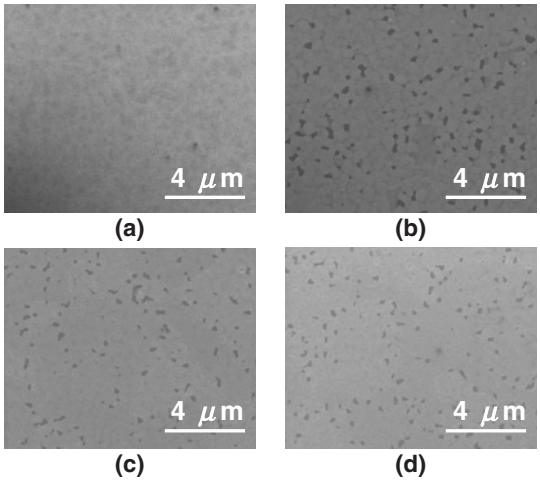

Fig. 3. SEM images of the C0As35 samples with different silicide formation temperatures: (a) 600, (b) 700, (c) 750, and (d) 800 °C. Several holes are generated within the Ni-silicide film at 700 °C, causing an increase in sheet resistance.

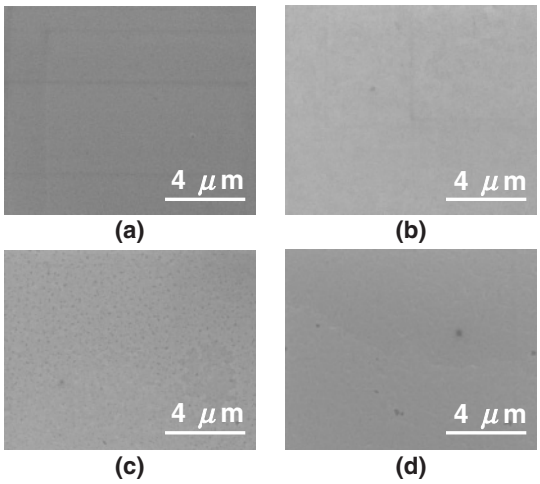

Fig. 4. SEM images of the C1As35 samples with different silicide formation temperatures: (a) 600, (b) 700, (c) 750, and (d) 800 °C. Only a few small holes can be observed at 750 °C.

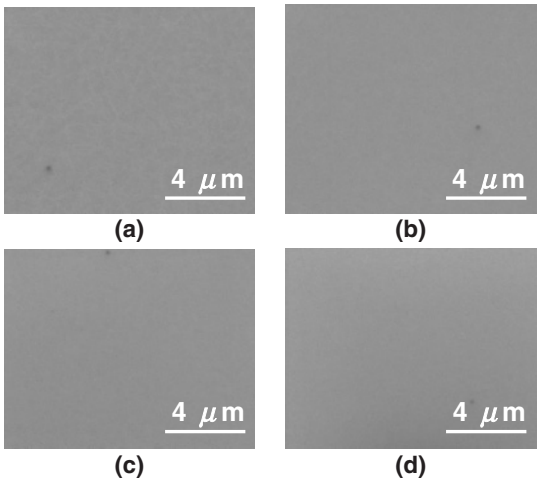

Fig. 5. SEM images of the C5As35 samples with different silicide formation temperatures: (a) 600, (b) 700, (c) 750, and (d) 800 °C. No holes can be observed, and the Ni-silicide film retains an intact structure.

increase from 700 °C because of NiSi film agglomeration. Many broken holes in the NiSi film can be seen in Fig. 3(b). On the other hand, few holes can be observed at 750 °C in the C1As35 samples, as shown in Fig. 4(c), and a continuous Ni-silicide film without any holes is obtained even at 800 °C in the C5As35 samples, as shown in Fig. 5(d). Hence, it is confirmed that sufficient C atoms can effectively suppress the agglomeration of Ni-silicide film.

To understand the reason for the increased R_s values of the C1As35 samples at 750 °C and the C5As35 samples at 800 °C, XRD analysis was used to identify the Ni-silicide phase. The XRD spectra of C1As35 and C5As35 samples are shown in Figs. 6(a) and 6(b), respectively. In Fig. 6(a), it is observed that the $NiSi_2$(400) phase appears at 750 °C in the C1As35 samples, and the NiSi(121) phase coexists in the Ni-silicide film at the same time. Furthermore, the NiSi(121) phase disappears and only the $NiSi_2$(400) phase can be detected at 800 °C. In the C5As35 samples, the $NiSi_2$(400) phase does not occur until 800 °C, as shown in Fig. 6(b). According to these observations, it is clear that increasing the C I/I dose to $5 \times 10^{15}\,cm^{-2}$ can retard the phase transformation of NiSi film. In summary, performing the C I/I process with a higher C dose of $5 \times 10^{15}\,cm^{-2}$ is a feasible method for enhancing the thermal stability of NiSi film even if As dopants exist.

Figure 7 shows the measured R_s values as a function of silicide formation temperature with As I/I energy at 85 keV, and the corresponding SEM images and XRD spectra are shown in Figs. 8 and 9, respectively. The information revealed from these figures is similar to that discussed previously. Moreover, the phase transformation temperature of the C0As85 samples is 750 °C while that of the C0As35 samples is 700 °C. On the basis of the experimental results of Ahmet *et al.*,[17] we consider that the higher As I/I energy results in fewer As dopants within the NiSi film. Thus, the phase transformation temperature of the C0As85 samples is 50 °C higher than that of the C0As35 samples.

The agglomeration temperature and phase transformation temperature of all samples are summarized in Table II. It is clear that C I/I with a dose of $1 \times 10^{15}\,cm^{-2}$ can raise the

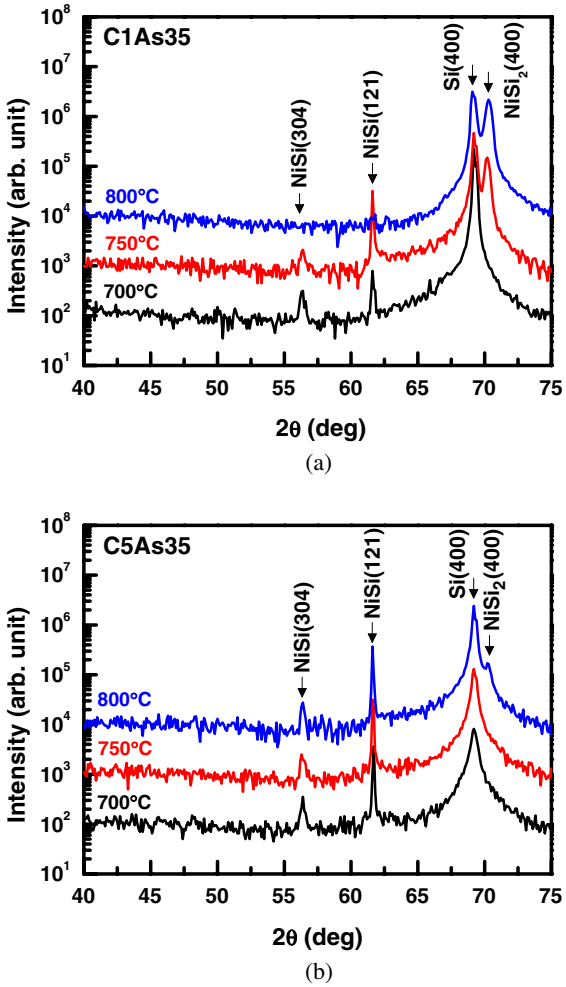

Fig. 6. (Color online) XRD spectra of the (a) C1As35 and (b) C5As35 samples. The $NiSi_2$ phase appears to cause an increase in the sheet resistance at 750 °C in the C1As35 samples and at 800 °C in the C5As35 samples.

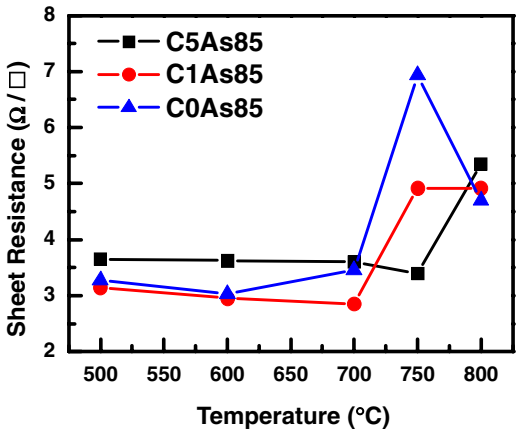

Fig. 7. (Color online) Sheet resistance values as a function of silicide formation temperature with As I/I energy at 85 keV and different C I/I doses.

agglomeration and phase transformation temperatures of Ni-silicide film to 750 °C. By increasing the C I/I dose to $5 \times 10^{15}\,cm^{-2}$, the phase transformation temperature of Ni-silicide film can be further raised to 800 °C, and the agglomeration temperature becomes higher than 800 °C.

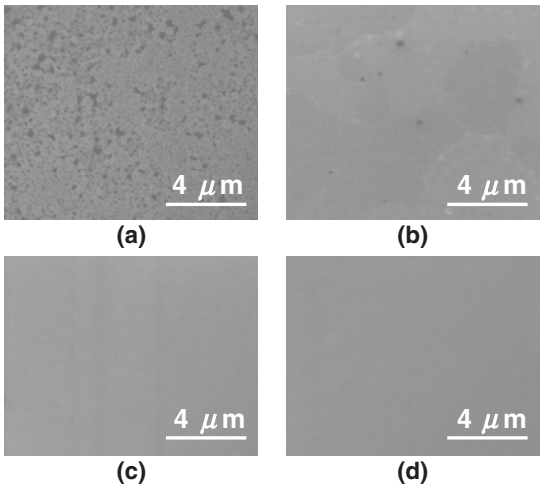

Fig. 8. SEM images at agglomeration temperature with As I/I energy at 85 keV and various C I/I doses: (a) C0As85 at 700 °C, (b) C1As85 at 750 °C, (c) C5As85 at 750 °C, and (d) C5As85 at 800 °C.

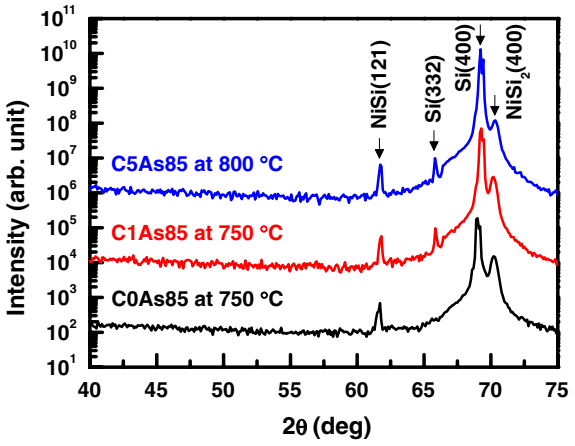

Fig. 9. (Color online) XRD spectra at phase transformation temperature with As I/I energy at 85 keV and various C I/I doses.

Table II. Summary of results of agglomeration and phase transformation temperatures of all samples.

Sample ID	Agglomeration temperature (°C)	Phase transition temperature (°C)
C5As35	>800	800
C1As35	750	750
C0As35	700	700
C5As85	>800	800
C1As85	750	750
C0As85	700	750

The C I/I process successfully enhances the thermal stability of Ni-silicide film by at least 100 °C.

3.2 Junction characteristics

Figure 10 shows the *I–V* characteristics of the Ni-silicide-contact n^+/p shallow junction with As I/I energy at 35 keV. The junction area is 6.25×10^{-4} cm^2. Both the C1As35 and C5As35 samples exhibit the lowest leakage current at the silicide formation temperature of 500 °C. The lowest leakage value is approximately 10 nA/cm^2 at a reverse bias of 3 V, and this value is close to that of the junction without silicide.

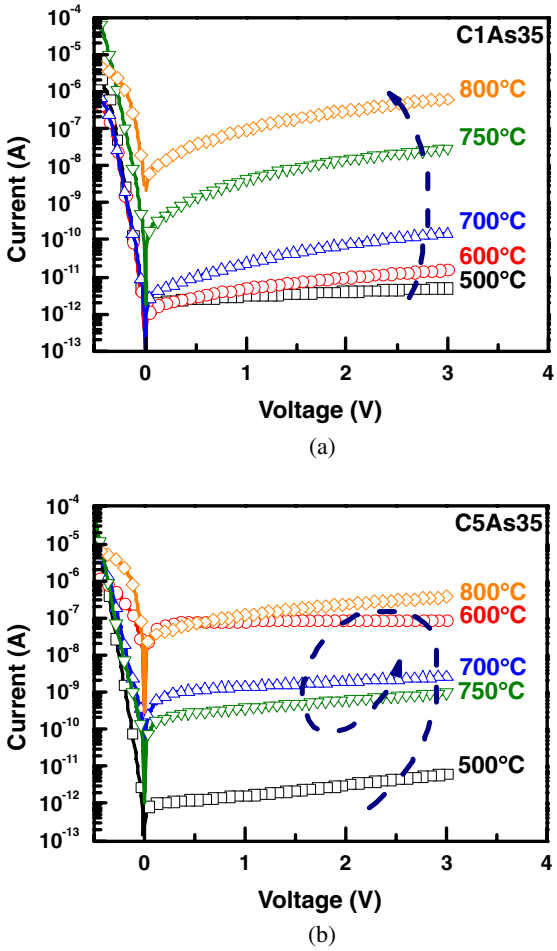

Fig. 10. (Color online) Silicide formation temperature dependences of leakage current characteristics of Ni-silicide-contact n^+/p shallow junction with As I/I energy at 35 keV: (a) C1As35 and (b) C5As35 samples.

For the C0As35 and C1As35 samples, the leakage current increases with increasing silicide formation temperature. However, the samples with a C I/I dose of 5×10^{15} cm^{-2} exhibit very different reverse leakage current behavior. For the C5As35 samples, when the silicide formation temperature increases to 600 °C, the leakage current abruptly increases by 3 orders of magnitude. Then, the leakage current decreases as the silicide formation temperature increases to 700 and 750 °C, but increases again as the silicide formation temperature increases to 800 °C. Figures 11 and 12 show statistics of the junction leakage current at a reverse bias of 3 V for the Ni-silicide-contact n^+/p shallow junctions with As I/I at 35 and 85 keV, respectively. The silicide formation temperature dependences of the junction leakage current described above are confirmed to be universal behavior. The same leakage current dependence on the silicide formation temperature and C I/I dose can also be found at an As I/I energy of 85 keV, as shown in Fig. 12.

Three mechanisms are considered to have an effect on the junction leakage current. The first one is the agglomeration of the Ni-silicide film. Agglomeration causes an increase in interface roughness at the Ni-silicide/Si contact, and the junction leakage current may increase owing to structural damage. The second is the diffusion of Ni atoms. The many defects produced by the high-dose I/I process form the

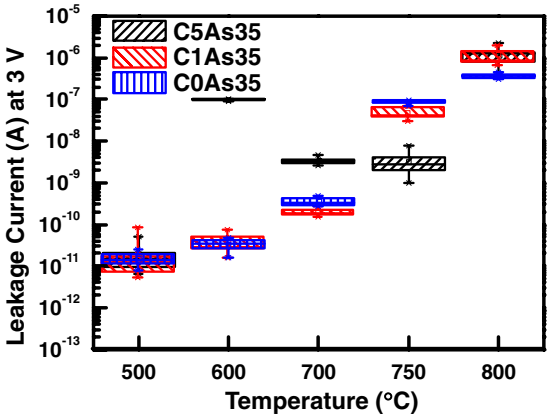

Fig. 11. (Color online) Statistics of the reverse-bias junction leakage current at 3 V for the Ni-silicide-contact n^+/p shallow junctions with As I/I at 35 keV.

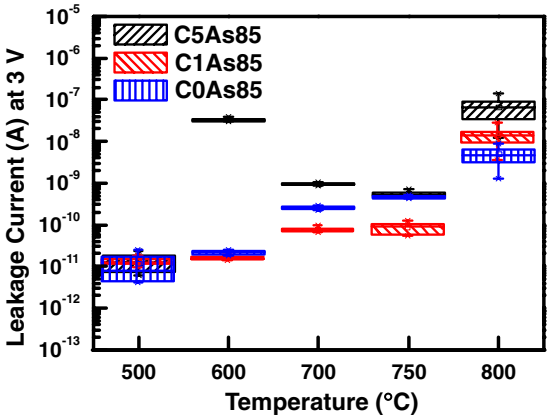

Fig. 12. (Color online) Statistics of the reverse-bias junction leakage current at 3 V for the Ni-silicide-contact n^+/p shallow junctions with As I/I at 85 keV.

diffusion path. Ni atoms can rapidly diffuse via these defects during silicide formation. As Ni atoms diffuse toward the junction depletion region and form deep levels, the junction leakage current increases. The third is the phase transformation from the NiSi phase to the $NiSi_2$ phase. When the phase transformation occurs, the thickness of the silicide film becomes double that of the NiSi film. Thus, the Ni-silicide/Si interface becomes closer to the junction depletion region. Agglomeration can easily damage the junction depletion region, and more Ni atoms can arrive at the junction depletion region to contribute to the junction leakage current. Agglomeration and the phase transformation occur at a high silicide formation temperature and depend on the silicide formation temperature and C I/I dose. In addition to the silicide formation temperature, the effect of the diffusion of Ni atoms is also related to the number of I/I defects, which depends on the C I/I dose.

For the reasons mentioned above, the deeper junction has fewer Ni atoms within the junction depletion region. Moreover, the agglomeration and phase transformation also have less impact on the deeper junction. Hence, by comparing Figs. 11 and 12, it can be seen that the leakage current at an As I/I energy of 85 keV is much lower than that at 35 keV at a high silicide formation temperature.

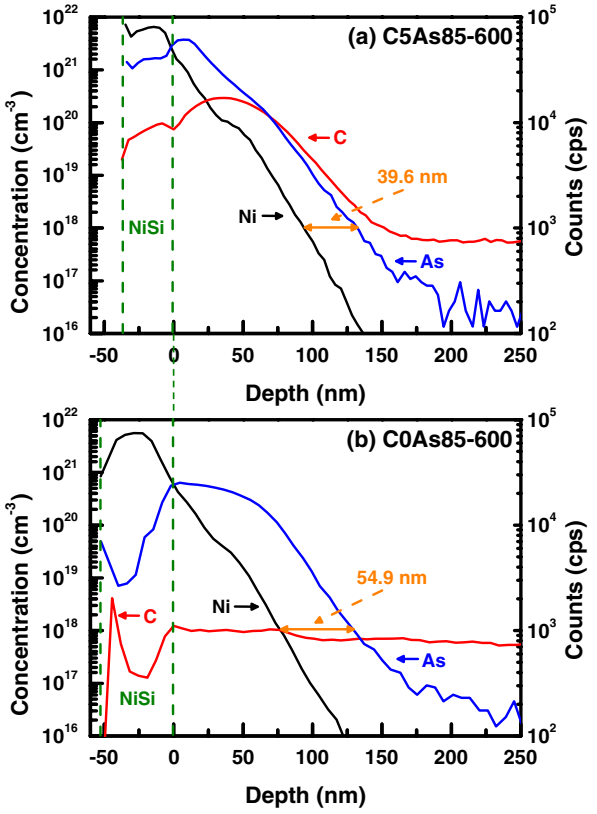

Fig. 13. (Color online) SIMS depth profiles of C, Ni, and As of the (a) C5As85 and (b) C0As85 samples with silicide formation temperature at 600 °C.

When the C I/I dose is zero or equal to $1 \times 10^{15}\,cm^{-2}$, the number of defects is not large enough to form a long diffusion path for Ni atoms. Hence, the agglomeration and phase transformation dominate the junction leakage current mechanism, and the junction leakage current increases with silicide formation temperature. Because the C1As35 and C1As85 samples have better thermal stability of the Ni-silicide film, both samples exhibit a lower leakage current than the C0As35 and C0As85 samples with silicide formation temperatures of 700 and 750 °C.

On the other hand, when the C I/I dose increases to $5 \times 10^{15}\,cm^{-2}$, it generates many remnant defects, and Ni atoms can diffuse very rapidly via these defects. Therefore, the diffusion of Ni atoms dominates the junction leakage current mechanism. The leakage currents of the C5As35 and C5As85 samples are similar to that of the C0As35 sample at 500 °C, as can be observed by comparing Figs. 11 and 12. This indicates that most of the defects generated by a high C I/I dose were annihilated by RTA at 1100 °C for 30 s. Figures 13(a) and 13(b) show the secondary ion mass spectrometer (SIMS) depth profiles of C, As, and Ni atoms of the C5As85 and C0As85 samples with the silicide formation temperature at 600 °C, respectively. The different surface NiSi thicknesses of these two samples is due to the thickness variation of the as-deposited Ni films. Hence, all of the depth profiles were measured from the NiSi/Si interface, which is defined as the intersection of the Ni and As depth profiles. Rucker *et al.* reported that substitutional C atoms can enhance As dopant diffusion, but the diffusion enhancement effect ends when most of the C atoms precipitate.[18] In

the case of our C5As85 samples, C atoms were incorporated by I/I, and this process produced a large number of Si interstitials. It is well known that C atoms can trap Si interstitials to eliminate secondary defects during high-temperature annealing.[19] Hence, C atoms combine with Si interstitials and precipitate to form immobile clusters during high-temperature annealing. Compared with the epitaxial Si:C layer in Rucker *et al.*'s experiment, most of the C atoms are not located at substitutional sites in our C5As85 samples. Therefore, no As diffusion enhancement is observed upon comparing Fig. 13(a) with Fig. 13(b). It is observed that the Ni depth profile of the C5As85 sample has an apparent hump whose position coincides with the peak of the C depth profile. The distance between As and Ni atom depth profiles measured at an As atom concentration of $1 \times 10^{18}\,\mathrm{cm}^{-3}$ is indicated in Figs. 13(a) and 13(b). The Ni distribution of the C5As85 sample is about 15 nm closer to the n^+/p junction than that of the C0As85 sample. This implies that the C5As85 sample has more Ni atoms within the junction depletion region owing to the dissolution and diffusion of Ni atoms toward the junction depletion region along the many defects induced by C I/I with a dose of $5 \times 10^{15}\,\mathrm{cm}^{-2}$ during silicide formation. This explains why the C5As35 and C5As85 samples unexpectedly exhibit the highest leakage current at 600 °C. We consider that the Ni-silicide formation process can generate more and more vacancies injecting into the Si substrate at a higher temperature.[20] Some residual defects can be combined and removed by these vacancies, so that fewer Ni atoms can diffuse into the junction depletion region. Therefore, the junction leakage current decreases as the silicide formation temperature increases to 700 and 750 °C. Finally, the increase in the leakage current again at 800 °C is a result of the agglomeration and phase transformation of the Ni-silicide film.

To suppress the diffusion of nickel atoms, we propose two solutions. One method is to ensure that the C distribution is shallower than the junction depletion region by introducing a lower C I/I energy. Thus, a higher concentration of C atoms near the Si substrate surface can be obtained. We predict that this will further enhance the thermal stability of the nickel silicide film. Furthermore, defects are far away from the junction, thus reducing the leakage current. The other method is to eliminate the defects as completely as possible. Raising the thermal budget of RTA or developing other annealing processes to eliminate these defects will be researched in the future.

4. Conclusions

We have investigated the impact of carbon ion implantation on the thermal stability of nickel-silicide film and nickel-silicide-contact n^+/p shallow junctions for the first time. It is verified that the carbon ion implantation process is indeed useful for improving nickel silicide thermal stability at high temperatures, regardless of whether arsenic dopants exist. Improved efficiency depends on the quantity of the carbon ion implantation dose. A sufficient dose of carbon atoms of $5 \times 10^{15}\,\mathrm{cm}^{-2}$ can effectively suppress the agglomeration and phase transformation of the nickel silicide film. According to our experimental results, the increases in the agglomeration and phase transformation temperatures reach at least 100 °C. Although carbon atoms existing within the nickel silicide film may increase the sheet resistance at a low silicide formation temperature ($\leqq$700 °C) owing to the segregation of carbon atoms at the grain boundaries, this only results in slightly larger sheet resistance values.

The leakage current mechanisms of nickel-silicide-contact n^+/p shallow junctions are also explained in detail in this paper. Good thermal stability of the nickel silicide film and better junction *I–V* characteristics cannot be obtained at the same time. A higher carbon ion implantation dose of $5 \times 10^{15}\,\mathrm{cm}^{-2}$ causes numerous defects, and nickel atoms diffuse very rapidly along these defects into the junction depletion region. Therefore, the leakage current suddenly increases owing to the existence of deep levels, i.e., nickel atoms.

Acknowledgements

The authors would like to thank the Nano Facility Center of National Chiao-Tung University, National Nano Device Laboratories for providing the experimental facilities, and the MHII Lab. of National Cheng Kung University for assistance with the carbon ion implantation process. This work was supported by the National Science Council, Taiwan, R.O.C. under contract No. NSC-96-2628-E-009-167-MY3 and the National Nano Device Laboratories under contract No. NDL97-C05M2G-016.

1) H. Iwai, T. Ohguro, and S. I. Ohmi: Microelectron. Eng. **60** (2002) 157.
2) T. H. Hou, T. F. Lei, and T. S. Chao: IEEE Electron Device Lett. **20** (1999) 572.
3) D. Mangelinck, J. Y. Dai, J. S. Pan, and S. K. Lahiri: Appl. Phys. Lett. **75** (1999) 1736.
4) P. S. Lee, K. L. Pey, D. Mangelinck, J. Ding, A. T. S. Wee, and L. Chan: IEEE Electron Device Lett. **21** (2000) 566.
5) L. W. Cheng, S. L. Cheng, L. J. Chen, H. C. Chien, H. L. Lee, and F. M. Pan: J. Vac. Sci. Technol. A **18** (2000) 1176.
6) A. S. W. Wong, D. Z. Chi, M. Loomans, D. Ma, M. Y. Lai, W. C. Tjiu, S. J. Chua, C. W. Lim, and J. E. Greene: Appl. Phys. Lett. **81** (2002) 5138.
7) R. T. P. Lee, D. Z. Chi, M. Y. Lai, N. L. Yakovlev, and S. J. Chua: J. Electrochem. Soc. **151** (2004) 642.
8) S. Zaima, O. Nakatsuka, A. Sakai, J. Murota, and Y. Yasuda: Appl. Surf. Sci. **224** (2004) 215.
9) O. Nakatsuka, K. Okubo, A. Sakai, M. Ogawa, Y. Yasuda, and S. Zaima: Microelectron. Eng. **82** (2005) 479.
10) R. T. P. Lee, L. T. Yang, T. Y. Liow, K. M. Tan, A. E. J. Lim, K. W. Ang, D. M. Y. Lai, K. M. Hoe, G. Q. Lo, G. S. Samudra, D. Z. Chi, and Y. C. Yeo: IEEE Electron Device Lett. **29** (2008) 89.
11) Y. Liu, O. Gluschenkov, J. Li, A. Madan, A. Ozcan, B. Kim, T. Dyer, A. Chakravarti, K. Chan, C. Lavoie, I. Popova, T. Pinto, N. Rovedo, Z. Luo, R. Loesing, W. Henson, and K. Rim: Symp. VLSI Tech. Dig., 2007, p. 44.
12) S. M. Koh, K. Sekar, D. Lee, W. Krull, X. Wang, G. Samudra, and Y. C. Yeo: IEEE Electron Device Lett. **29** (2008) 1315.
13) A. C. Mocuca and D. W. Greve: J. Appl. Phys. **85** (1999) 1240.
14) K. W. Ang, K. J. Chui, V. Bliznetsov, A. Du, N. Balasubramanian, M. F. Li, G. Samudra, and Y. C. Yeo: IEDM Tech. Dig., 2004, p. 1069.
15) K. W. Ang, K. J. Chui, V. Bliznetsov, Y. Wang, L. Y. Wong, C. H. Tung, N. Balasubramanian, M. F. Li, G. Samudra, and Y. C. Yeo: IEDM Tech. Dig., 2005, p. 497.
16) B. Y. Tsui and C. P. Lin: IEEE Trans. Electron Devices **52** (2005) 2455.
17) P. Ahmet, T. Shiozawa, K. Nagahiro, T. Nagata, K. Kakushima, K. Tsutsui, T. Chikyow, and H. Iwai: Microelectron. Eng. **85** (2008) 1642.
18) H. Rucker, B. Heinemann, and R. Kurps: Phys. Rev. B **64** (2001) 073202.
19) S. Nishikawa and T. Yamaji: Appl. Phys. Lett. **62** (1993) 303.
20) L. J. Chen: *Silicide Technology for Integrated Circuits* (IEE, London, 2004) p. 27.